3
Fabrication and characterization

This chapter briefs about all the fabrication steps and characterization techniques used for fabricating the spectrally selective absorber coatings and their characterization.

3.1 Substrates cleaning

Cu and SS substrates were first metallographically polished by 2000 grade silicon carbide (SiC) abrasive paper to remove the surface roughness and impurities present on the substrate surface. Then, this mechanically cleaned substrate is cleaned using trichloroethelene at 80 °C for 5-10 minutes and rinse with water. Further, the substrates were cleaned in acetone at 80 °C for 5-10 minutes and rinse with water. At each step, substrate was rinsed with DI water. Finally, substrates are exposed to dry nitrogen gas for drying before the deposition. In the case of Ni, Co co-deposition, the aluminum substrates of size 80 × 40 × 1 mm^3 were chemically cleaned in a basic solution containing NaOH (5g L^{-1}), $Na_2Co_3.6H_2O$ (5 g L^{-1}), $Na_2SiO_3.5H_2O$ (1 g L^{-1}) for one minute. Then, in the second step, the substrate was cleaned in NaOH (25g L^{-1}) solution for a duration of one minute, and in the last step, the substrate was neutralized in acidic solution containing HNO_3 (20%V/V) for the duration of 2 minutes. After each step, substrates were properly rinsed by DI water and finally dried in the flow of N_2 gas.

3.2 Fabrication methodology for spectrally selective absorber coating

The spectrally selective absorber coatings in this thesis work are deposited using electrodeposition, thermal evaporation, and sol-gel based spin and dip coating. For depositing an IR layer, sputtering is used. The properties of the fabricated structure to a great extent, depend on the deposition techniques. The present section gives a critical review of the widely adopted deposition techniques for the development SSAC layer, IR reflecting layer, and their impact on selective optical properties.

3.2.1 Silver and Black chrome coating

3.2.1.1 Thermal evaporation of Silver

There are numerous techniques for coating a metallic surface using physical vapor deposition (PVD) route such as DC/RF sputtering, chemical vapor deposition, and thermal/electron-beam evaporation. The thermal evaporation process is preferred for low melting temperature materials due to adherence of metallic thin film on a substrate, a high deposition rate, and surface roughness. The deposition process is scalable over a large area without compromising the film quality and economical. Because of these advantages, thermal evaporator system made by Semicore Triaxis is used to deposit a silver thin film on reflecting surface. The deposition of the thin film was optimized on a flat copper substrate of size 2.5 cm × 2.0 cm to get high reflectance in the solar spectrum range (Uv-Vis). Finally, the silver thin film is deposited on the reflector part of the radiation calorimeter (RADCAL). Before the deposition, the chamber pressure was maintained at approximately 3.0 x 10^{-6} torr. The silver source material

of 99% purity was used for deposition. The DC power of 3.46 kW was supplied to the tungsten boat filled with the silver source to evaporate. The source was fixed at 20 cm below the substrate. The depositing silver growth rate was monitored by a quartz crystal. Finally, the silver thin film with optimized condition deposited on the conical reflecting surface of RADCAL. **Figure 3.1** shows the schematic image of the thermal evaporator system used for silver deposition.

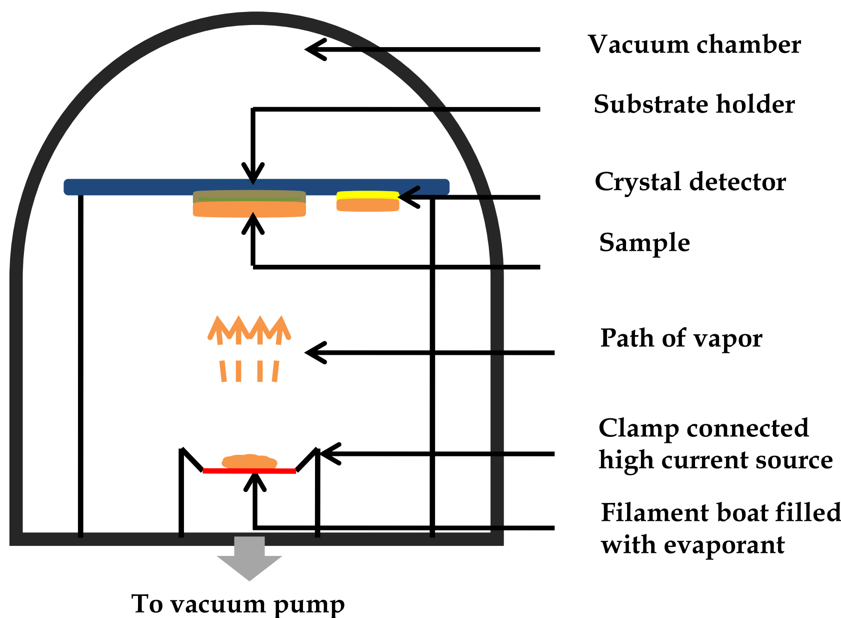

Figure 3.1: The schematic of thermal evaporator used for silver deposition

3.2.1.2 Black chrome electrodeposition

Before black chrome deposition, Ni as an IR layer electrodeposited on cleaned Cu substrate. The cleaning of Cu substrate is explained in section **3.1.** The electrochemical solution contains nickel sulfate and nickel chloride prepared. The primary source Ni^{2+} ion in the bath is NiSO4, whereas NiCl is used for the homogeneous distribution of Ni^{2+} ion for uniform deposition purpose. Boric acid is added in solution mixture to control the PH. The amount of mixed chemical to prepare solution is given in detail in **Table 3.1.** Electrodeposition of Ni carried out at a current density of 0.085A/cm^2. Nickel electrodeposited on Cu substrate by reduction of Ni^{2+} ion in four steps (Saraby-Reintjes & Fleischmann, 1984). The detailed Ni probable electrodeposition mechanism is given in the left column of **Table 3.1.**

Black chrome electrodeposited on Ni coated Cu substrate. The current density range used for the BC deposition was 0.2 A/cm^2 – 0.5 A/cm^2. In the present case, the depositing surface was very high ~ 86 cm^2. So the total current required for this deposition was in the range of 17.2-43A. Deposition at such a high current may affect the electrochemical solution, which may degrade the characteristic of the absorber layer. The electrochemical solution for black chrome deposition prepared by mixing chromium oxide, sodium fluoride, and sodium nitrate. The detail bath and deposition condition summarized in the right column of **Table 3.2.** In the bath, chromium oxide is the main source of Cr^{6+} ion. The NaF and $NaNO_3$ are used to catalyze the electrodeposition reaction. The detailed chemical reaction mechanism of Ni and BCC electrodeposition is given in detail in **Table 3.2.**

A representative electroplating diagram is shown in **Figure 3.2 (a)** with the respective layer stack in **Figure 3.2 (b)** comprising an infrared nickel reflector and a black chrome spectral selective absorber.

Table: 3.1. Experimental detail for Ni and Cr-Cr2O3 (BC) electrodeposition

Experimental detail for Ni electrochemical deposition		Experimental detail for BC electrochemical deposition	
$NiSO_4.6H_2O$	250 g/l	CrO_3	275 g/l
$NiCl_2.6H_2O$	60 g/l	NaF	0.2 g/l
H_3BO_3	40 g/l	$NaNO_3$	3 g/l
Temperature:	40 °C	Temperature:	15-17 °C
Time (t)	30 s	Time (t)	60 s
Current density (J)	0.000 85 A/mm^2	Current density (J)	0.003 A/mm^2

Table3.2. Reaction mechanism for Ni and Cr-Cr_2O_3 deposition

Ni electrodeposition	Cr-Cr_2O_3 electrodeposition
$Ni_2 + Cl- \longrightarrow NiCl^+$ $NiCl^+ + e- \longrightarrow NiCl$ $NiCl + e- \longrightarrow NiCl_{ads}$ $NiCl_{ads} + e- \longrightarrow Ni + Cl^-$	$HCr_3O_{10}^- + 6H^+ + 6e- \rightarrow Cr_2O_3 + HCrO_4 + 3H_2O$ $HCr_3O_{10}^- + 2H_2O \leftrightarrow Cr(OH)_2 + HCr_2O_7^- + 2HF + H^+$ $Cr(OH)_2 \leftrightarrow CrO + H_2O$ $CrO + HF \overset{HF}{\leftrightarrow} Cr + H_2O$

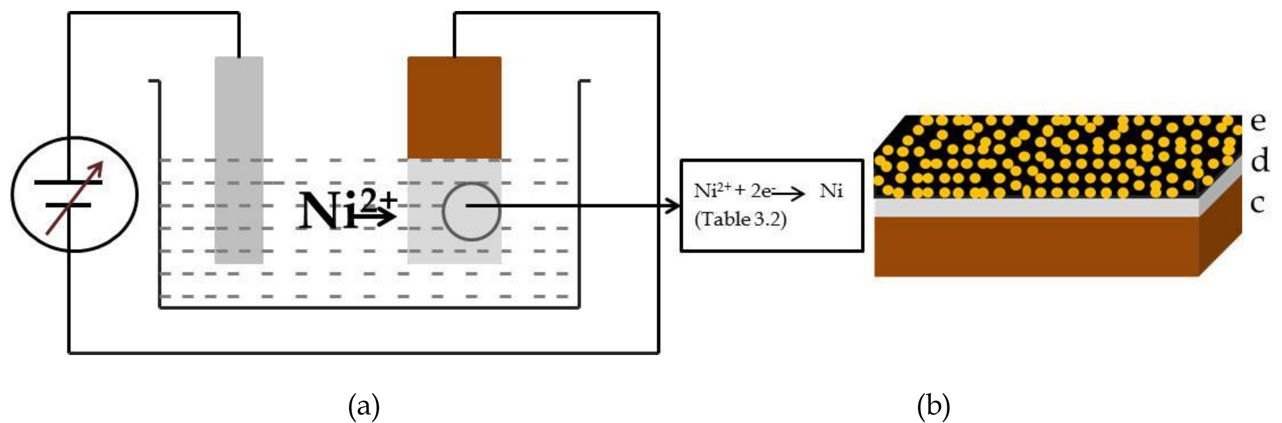

Figure 3.2 (a) Electrodeposition experimental schematic of nickel and black chrome layers and (b) Schematic of electrodeposited black chrome on Ni deposited Cu substrate (BC/Ni/Cu)

3.2.2 Ni, Co co-deposition on nanoporous anodized alumina

The cleaned aluminum substrates of size 80 × 40 × 1 mm3 size are used for anodization. The cleaning procedure explained in section 3.1. Here the aluminum substrate and graphite sheet of size 7×10×3 mm^3 are used as working and counter electrode, respectively [Boström et al., 2003, Green et al., 2007]. The anodization reaction carried out in an electrochemical bath of 2M phosphoric acid for 15 minutes at 15 V DC potential at room temperature. Ni and Co electrodeposition on anodized alumina substrate is carried out in an electrochemical bath solution containing $CoSO_4$ (0.11M), $NiSO_4$ (0.11M), H_3BO_3 (0.2M) and ascorbic acid (0.1M) at 10 V_{ac} potential. For optimization, several samples were deposited by varying the deposition time duration [Cuevas et al., 2014, Foyet et al., 2008].

3.2.3 W as IR layer On SS substrate using sputtering

W thin film on cleaned stainless steel (SS) substrate of size 2.5 x 2.5 cm^2) carried out using the sputtering system in DC power configuration. During optimization to get thin fill with minimized thermal emittance, several films were deposited by very different deposition parameters like duration, temperature, and power applied. The substrate cleaning procedure is mentioned in **section 3.1.** The substrate holder of size 6′ is placed in a vacuum chamber with a cleaned substrate mounted on it for W deposition. A high purity (99.9%) tungsten target of 101.6 mm dia and 6.35 mm thick size mounted on target holder. The vacuum level of the chamber was down to 5.0–6.0 × 10^{-6} mbar after loading the chamber to minimize the oxygen impurity. Before tungsten thin film deposition, the deposition chamber heated at 450°C for 2-hour duration at 5.0–6.0 × 10^{-6} mbar chamber pressures. Also, the pre-sputtering of the tungsten target is done for 10 minutes for target surface cleaning. For deposition, the rate of argon gas flow was 50 sccm. During deposition, the working pressure of the chamber was 2.0 (± 0.1) × 10^{-2} mbar. For optimization purposes to get the film with lowest thermal emittance, several samples were deposited by changing in deposition conditions such as DC power, deposition duration, and temperature. **Figure 3.3**.shows the schematic of RF/DC sputtering system

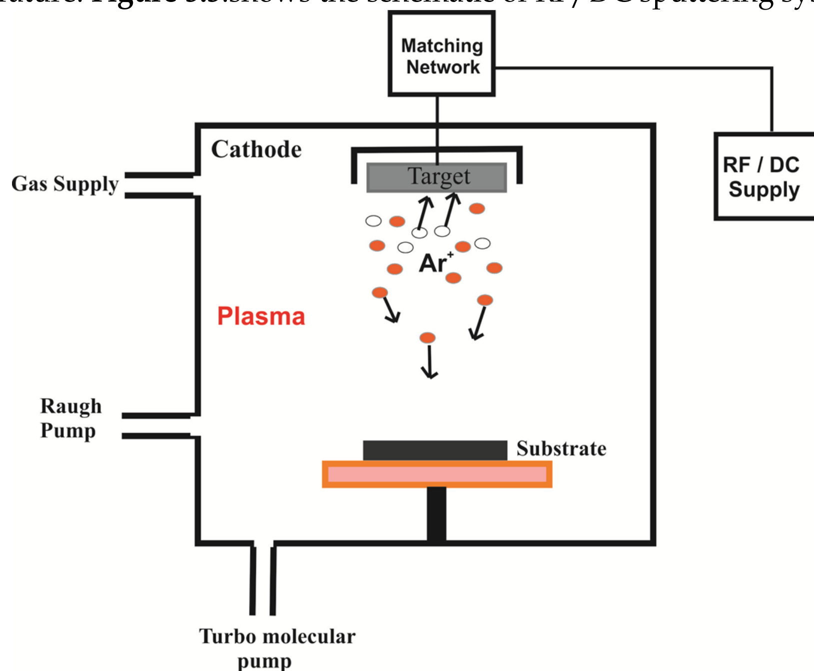

Figure 3.3 RF/DC sputtering system schematic image

3.2.4 $SiO_2/(ZnO/Sn\text{-}In_2O_3)_{n=4}/SS$ using sol-gel dip coating

The stable solution for In_2O_3 thin films is prepared by adding 2.8 g of indium nitrate in 40ml 2-methoxy ethanol and 1.6 ml acetylacetone. Further, 520 µl nitric acid (HNO_3), followed by 520 µl of ammonium hydroxide (NH_4OH) is added slowly in the indium nitrate precursor solution. After ensuring the complete mixing, 920 µl NH_4OH is added in the solution, which is kept for continuous 12 hours stirring to get the final indium oxide sol. ZnO solution is prepared similarly by replacing indium nitrate by zinc nitrate, following similar steps. For the preparation of SiO_2 solution, 60ml of C_2H_5OH, 4ml MOES and 1ml TEOS mixed. HCl is added dropwise to fixed solution at pH 2. The mixture solution kept for stirring at 80 °C for 10 minutes. Stainless steel 304 sheets (3 cm × 3 cm square) are used as substrates. The substrate surface roughness and contamination were removed using the emery paper of 2000 grade. The substrate is further subjected to the chemical cleaning by first keeping it in trichloroethylene and then acetone at 80 °C for 5-10 minutes. After that, the substrate is properly rinsed in deionized water and dried using nitrogen gas flow. These cleaned SS substrates were used for any layer deposition. Tin

doped In_2O_3 layer followed by ZnO layer is deposited on the SS substrate by dip coating. Each layer is dip-coated at 2mm/sec dipping and removing speed, followed by 5 min air drying at 300°C. A set of such four In_2O_3 followed by ZnO layers is deposited on the SS substrate. In the end, on top SiO_2 layer coated as anti-reflecting coating. For the deposition, a dip coating system is indigenously developed, and details are given in **Annexure A**. After deposition of complete multilayer structure, the coted film was kept at 450°C for 3 hours to crystallize and remove organic impurities.

3.3 characterization of the fabricated sample

The structural study of fabricated samples was performed by XRD measurement. Microstructural analysis was performed using a scanning electron microscope. Elemental analysis was also carried out by energy dispersive X-Ray (EDX) measurement provided with SEM. To estimate the surface morphological structure, atomic force microscopy measurement was done. Raman spectroscopy analysis of the fabricated sample carried out to signify the composition present in the sample. The optical properties of the film i.e. absorptance in UV-Vis range is carried out by Uv-Vis spectroscopy. FTIR spectrum was recorded, and measured reflectance was used to estimate the thermal emittance of the fabricated thin film. Corrosion behaviors for the fabricated film were analyzed by potentiodynamic electrochemical reaction and electrochemical impedance spectroscopy measurement. The detail of the characterization followed for thesis work is presented in detail in subsequent sub-sections. The characterization detail of this work is presented in subsequent sub-sections.

3.3.1 X-ray diffraction (XRD) technique fabricated sample

The stuctural peroperties, such as crystallographic phase, structure, and crystallite size of the fabricated samples, are investigated using XRD measurements. It was Wilhelm Conrad Rontgen, a German scientist who discovered the X-ray in 1885. X-ray is an electromagnetic radition in 0.01-100 A wavelength range. Max von Laue first observed material crystallinity beavior in 1912. X-rays are generated after collision of high-speed electrons with metallic target. The characteristic X-rays are generated when high-speed energetic elctrons strike and knockout the inner cell electrons from the metallic target. For X-ray generation, X-ray tube, consisting of a metallic target and thermonic source for electron generation, is used. For accelerating the electrons, high-volatge between the electrodes is applied. Target is cooled simultaneously during X-ray genaration. The produced X-ray pass through soller slit and collimated X-rays are collected. Then, the collimated beam is passed through a divergence slot and falls onto a sample placed in the sample holder. And finally, the X-ray beam differs from the sample collected by the detector.

For our sample, we used Bruker D 8 advanced X-ray powder with 1.54 Å Cu-Kα monochromatic X-ray. The detailed parameters of XRD measurement for the fabricated sample are explained in the concerned chapter. The image of XRD instrument, used for analysis at IIT Jodhpur, is shown in **Figure 3.4.**

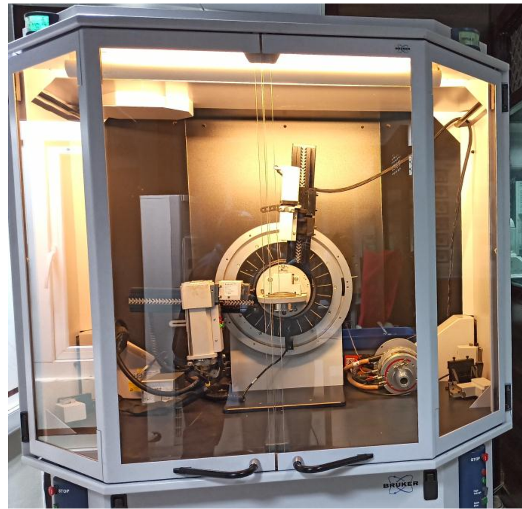

Figure 3.4 Camera image of X-ray Diffractometer at IIT Jodhpur

3.3.2 Scanning electron microscopy (SEM)

For the analysis of the microscopic surface structure, scanning electron microscopy (SEM) is used. In SEM mode, the focused high-energy electron beam scans the surface and, due to the interaction with the surface material, the generated signal is recorded. The generated signal includes secondary electrons, backscattered electrons, and X-rays. The secondary electrons are used for imaging, the backscattered electrons are used for the determination of the image with phase contrast, and the characteristic X-rays are used for the analysis of the elementary composition. The morphological surface information is obtained using the secondary electron, while the backscattered electron is used in the contrast of the image to specify the phase of a multiphase system. **Figure 3.5** shows the optical image of Carl Zeiss SEM EVO 18 used for capturing a surface image of the fabricated sample**.**

Figure 3.5 Optical image of scanning electron microscope used for amylases microscopic structure at IIT Jodhpur

3.3.3 Energy dispersive X-ray spectroscopy (EDX)

EDX spectroscopy analysis for elemental composition estimation carried out using EDX detector made by Oxford integrated with Carl Zeiss SEM EVO 18. It uses characteristic x-ray generated after the interaction of the electron with the material. Different element present in the specimen will generate different characteristic X-rays, which are separated in the form of the energy spectrum. Further, this spectrum was studied for elemental composition determination.

3.3.4 Atomic force microscope (AFM)

Atomic force microscopy measurements are carried out for surface morphological studies. In AFM, a tip attached to the cantilever, which scans the surface in 3-dimension. The physical fluctuation in tip during scanning converted into electrical signal by piezoelectric sensor attached to tip. In contact mode, the interaction force between tip and surface is repulsive. However, attractive force works in between tip and surface in non-contact mode. For comparatively rough surface, non-contact mode is preferred to avoid tip contamination and sample damage.

A scanning probe microscope (XE-70) made by Park is used to carry out topographical image analysis of a selective absorber surface. The surface roughness of the fabricated surface estimated using AFM measurement. The detail of AFM measurement of selective absorber surfaces is given in the result and discussion section of respective. **Figure 3.**6 is showing the image of the AFM instrument used at IIT Jodhpur.

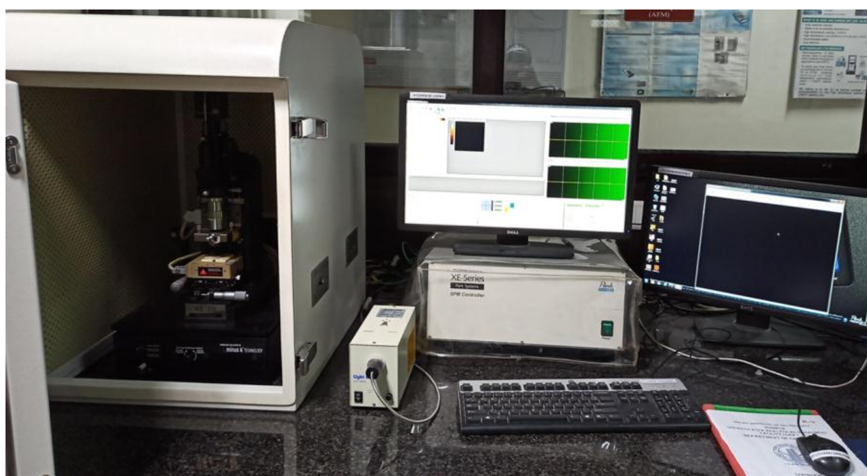

Figure 3.6 Optical image of scanning probe microscope (XE-70) at IIT Jodhpur

3.3.5 UV-Vis spectrophotometer

UV-Vis spectrophotometer (Agilent Cary 4000) is used to measure reflectance in UV-Visible range (0.2-0.9 µm). The total reflectance (diffuse plus specular) reflectance measured using DRA accessories provide with UV-Vis instrument. An integrating sphere made of polytetrafluoroethylene (PTFE) of 4mm thickness used to take reference in reflectance mode. The PTFE, a white material, is chosen for taking reference as it has very reflectance > 99% in 0.3 to 18µm range. It shows reflectance above 96% in 0.2 to 2.5 µm range. However, Agilent Carry-4000 UV-Vis spectrometer has only photomultiplier (PMT) detector, which can detect in the UV-Vis range. Then, reflectance measurement of the samples are carried out using the integrating sphere by mounting the sample on the reflectance port of the instrument. The integrated sphere can be connected in two positions: D and S. The D position only measure diffuse reflectance, whereas S position measures total reflectance (diffuse plus specular). **Figure 3.7** shows the UV-Vis instrument used for characterization at IIT Jodhpur.

Figure 3.7 Camera image of Cary 4000 UV- Vis spectrophotometer

3.3.6 Fourier Transform Infrared Spectrophotometer (FTIR)

The reflectance of the fabricated film in the infrared range (IR) measured using Bruker made FTIR spectrometer Vertex-70v. Generally, FTIR characterization carried out in transmittance mode to analyze vibration spectra of molecules due to change its molecular dipole moment. The Bruker FTIR vertex 70v provided with Triglycine sulfate detector, which is doped with Deuterated and L-alanine at room temperature. This FTIR spectrometer has very low resolution of 0.4 cm^{-1}. The reflectance of gold is taken as reference as it has very high reflectance in the infrared region. In this work, reflectance of selective absorber coating was measured in the infrared region (2.5 to 25 μm) to estimate the emittance. **Figure 3.8** shows the system used for FTIR measurement at IIT Jodhpur.

Figure 3.8 Optical image of FTIR spectrometer used for reflectance measurement at IIT Jodhpur

3.3.7 Raman spectroscopy

Raman spectroscopy measurement used for the analysis of inelastically scattered light produced due to interaction of molecular lattice vibrations in a material with the monochromatic radiation. In this work, Raman Microscope model name NomadicTM (Bay Spec, USA) used for measurement. In this instrument, different excitation sources (355 nm, 532 nm, and 785 nm), are available for Raman measurements. The dedicated optimized detector is provided for individual wavelength sources for resolution, sensitivity, and optical spectral coverage. To tune laser power, integrated laser control and motorized ND filters is also provide in this system. For the different modes of operation, like reflectance and transmittance, an optical microscope (Olympus) is used, which is integrated with the motor-driven stage. A microscope with a charged coupled device (CCD) camera on the top is provided for taking bright field images. The detail of Raman spectroscopy measurement for current work is given respective in chapter. **Figure 3.9** shows the image of the Raman spectroscopy measurement used at IIT Jodhpur.

Figure 3.9 Image of Raman spectrometer unit at IIT Jodhpur

3.3.8 Corrosion measurement

Corrosion is a naturally occurring process, where material, especially metal converted into its oxide, sulphide or hydroxide due to electrochemical and/or chemical reaction in open environmental conditions. It degrades the material and its properties. In this work, corrosion measurement of spectrally selective absorber coating is carried out to estimate the corrosion rate and on optical properties degradation. We did corrosion measurement analyzing using two electrochemical based techniques: one is electrochemical polarization, and another is electrochemical impendence spectroscopy measurement. Both measurements are performed in 3.5 % NaCl containing solution in three-electrode configuration. Autolab workstation (Metrohm) is used for corrosion measurements. The Ag/AgCl, platinum, and sample working as a reference, counter, and working electrode, respectively. To stabilize open circuit potential, in all measurement samples immersed in solution for 30 minutes duration. The OCP for each case was noted down. Further, the different corrosion parameters are calculated using Nova software provided with the electrochemical work station. In the electrochemical polarization technique, the corrosion resistance estimated using Stern–Geary relation (equation (3.1) [Stern and Geary, 1957]:

$$R_P = \frac{b_c \times b_c}{2.3 \times i_{corr}(b_c + b_a)} \qquad (3.1)$$

Where b_a and b_c denote anodic and cathodic curve slopes, respectively.

Further, in electrochemical impendence spectroscopy measurement carried out in a similar way using the FRA32 module of Autolab PGSTAT302N (Matrohm) in 0.1 Hz - 100 kHz range at 10mV AC voltage signal. The impendence measurements are performed at the respective open circuit potential of the system. The Nyquist plot (imaginary impendence versus real impendence and Bod plot (impendence magnitude versus frequency) are plotted and analyzed. The impendence spectrum is simulated with an equivalent circuit and best matched equivalent circuit of the respective sample is plotted. In the equivalent matched circuit R_s, R_p, and CPE (constant phase element) denotes solution resistance, polarization resistance and double layer capacitance, respectively. **Figure 3.10(a & b)** represents the schematic of electrochemical corrosion measurement and standard equivalent circuit. The detail of electrochemical polarization and impendence spectroscopy measurement is given in the result and discussion part of the respective chapter.

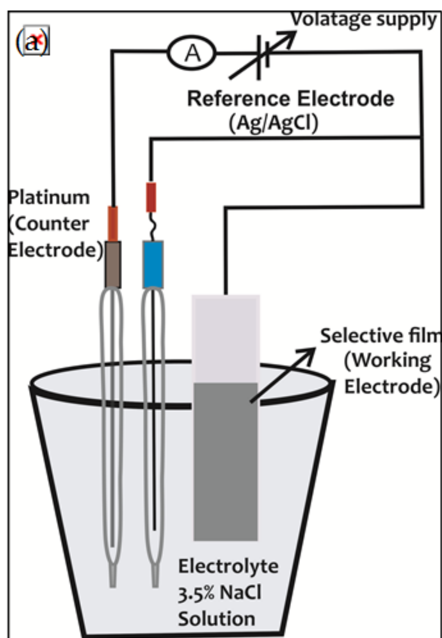

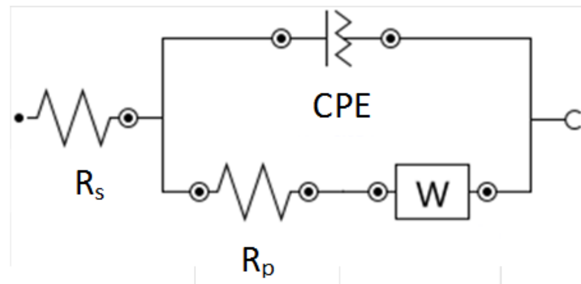

Figure 3.10 Schematic image of electrochemical polarization experiment for corrosion measurements